RESEARCH ARTICLE

Check for updates

Spatio-temporal variation of surface soil hydraulic properties under different tillage and maize-based crop sequences in a Mediterranean area

Rasendra Talukder [ID] · **Daniel Plaza-Bonilla** ·
Carlos Cantero-Martínez · Simone Di Prima ·
Jorge Lampurlanés

Abstract

Aims The surface crust formed by the drop impact of rainfall and/or irrigation is a prevalent characteristic in many Mediterranean soils. However, the temporal variation of soil hydraulic properties induced by surface crust during the high-frequency irrigation has rarely been investigated.

Methods Beerkan infiltration tests in conjunction with the BEST method were used to investigate the effects of surface crusting on the spatio-temporal variation of saturated soil hydraulic conductivity (K_s, mm s^{-1}), sorptivity (S, mm s$^{-0.5}$), mean pore size (r, mm), number of effective pores per unit area (N, m^{-2}) in Agramunt, NE Spain.

Results In response to autumn tillage, intensive tillage (IT) increased K_s and S due to higher r and N, but both declined after 60 days. Reduced tillage (RT), maintained comparable K_s and S values, despite having a lower N value. After the spring tillage, both IT and RT developed crusted layers, resulting in decreased K_s, S and N. Long-term no-tillage (NT) showed an increasing trend of K_s and S over time, except for the last sampling. Spatial variation (i.e., between the rows, B-row vs. within the row of crops, W-row) of K_s and S was found, and non-crusted soils (W-row) had consistently higher K_s and S than crusted soils (B-row).

Conclusions Conservation tillage i.e., RT and NT improve the surface soil structure and reduce the risk of crust development. Surface cover by crops may help to prevent crust formation within the row of crops, improving soil hydraulic conductivity.

Keywords Soil crust · Crop diversification · Conservation agriculture · Saturated hydraulic conductivity · Sorptivity · BEST method

Responsible Editor: Manuel T. Oliveira.

R. Talukder (✉) · J. Lampurlanés
Department of Agricultural and Forest Engineering, University of Lleida-AGROTECNIO-CERCA Center, Av. Rovira Roure 191, 25198 Lleida, Spain
e-mail: rasendra.talukder@udl.cat

D. Plaza-Bonilla · C. Cantero-Martínez
Department of Crop and Forest Sciences, University of Lleida-AGROTECNIO-CERCA Center, Av. Rovira Roure 191, 25198 Lleida, Spain

C. Cantero-Martínez · J. Lampurlanés
Associate Unit CSIC (Research Spanish Council), Zaragoza, Spain

S. Di Prima
School of Agricultural, Forestry, Food and Environmental Sciences (SAFE), University of Basilicata, 85100, Potenza, Italy

Introduction

Many soils, particularly in arable arid and semi-arid areas, form thin, compacted, dense surface layers

Ⓐ Springer

with lower porosities and higher bulk densities than the soils underneath (Neave and Rayburg 2007). These layers, also known as "structural crusts", are formed by two complex mechanisms i.e., (i) physical dispersion and (ii) chemical dispersion (Agassi et al. 1981). A physical dispersion of aggregates may happen, when soils are subjected to high-intensity water drops, whether by rain and/or irrigation. Since rainfall or irrigation began, the surface soil starts to wet rapidly, non-stable soil aggregates are broken and soil particles isolated, reorganized, and consolidated, clogging the pores, which in turn, form an unstructured layer. Further, splashing of fine particles transported in suspension by runoff in soil depressions and the subsequent drying form a thick soil layer (Badorreck et al. 2013). A chemical dispersion (or leaching of fine particles), on the other hand, is determined by the soil mineralogy, soil exchangeable sodium percentage (ESP), sodium absorption ration (SAR), and the electrolyte concentration (EC) of rain or irrigation water. The wet phase of this layer is referred as a "seal" and when dries is called "crust" (Moore and Singer 1990; Assouline 2004). Surface crusting is an indicator of land degradation for a variety of reasons. For instance, it impaired infiltration and percolation (Souza et al. 2014; Alagna et al. 2019), which generates runoff and erodes the soil surface (Wu et al. 2016), limiting solute and gas transport, seedling emergence, and root penetration (Baumhardt et al. 2004; Gabriel et al. 2021), and ultimately reducing crop yields (Souza et al. 2014; Ramos et al. 2019). Soil inherent properties like silt and clay content, and exchangeable sodium percentage increases the likelihood of soil sealing and crusting, while aggregate stability, organic matter content and electrolyte concentration reduces it (Agassi et al. 1981; Vandervaere et al. 1997; Šimůnek et al. 1998; Chen et al. 2013). Soils rich in silt and clay were found more prone to soil sealing with a low-intensity rainfall than sandy soils. When rain drops (distilled water) lowers the electrolyte concentration below the flocculation threshold at the soil surface, particle dispersion (and leaching) takes place and stimulate the soil sealing (Chen et al. 2013). Similarly, soils rich in quartz content significantly increases crust strength due to its inertness, which makes the soil highly dispersive (Nciizah and Wakindiki 2014). Beside this, soil with a high ESP (≥ 6.4) can promote particle dispersion, crust formation, and a significant decrease in

infiltration (Agassi et al. 1981), while an increase in EC decreases the chemical dispersion.

In addition, soil management practices have a substantial impact on surface soil crusting that is dependent on pedo-climatic conditions, soil textural type. For instance, Usón and Poch (2000) reported that crusting on a silty loam soils under rain-fed semiarid conditions was unaffected by tillage practices, whilst Palese et al. (2014) observed the opposite results on a sandy soils under rain-fed semiarid conditions (slope gradient was 0 to 16%). They noted that continuous IT made the soil much more vulnerable to crusting due to lower aggregate stability and reduced surface cover by crop residues (residue incorporation by tillage). In contrast, absence of disturbance (tillage) and surface cover by crop residues in NT reduced the risk of crusting. Furthermore, crop residues improve soil structural properties directly by preventing waterdrop impact and indirectly by promoting biological activity i.e., earthworms which help to create bio-channels and facilitating water flow. Crop sequences can also modify some soil properties related to soil crusting. For instance, cultivation of winter crop before summer crop can cover bare soil with living crops or residues, lowering water drop impact and protecting soils. In this regard, replacing the fallow season with a crop is a good practise for lowering soil crust development (Wu et al. 2016; Gabriel et al. 2021). Gabriel et al. (2021) reported that under irrigated condition replacemnet of bare fallow by cover crops (barley, *Hordeum vulgare L.*, or vetch, *Vicia sp. L.*) together with summer crops (maize, *Zea mays* L., or sunflower, *Helianthus annuus* L.) enhanced the soil surface conditions and prevent the crust formation under reduced tillage in a long-term field experiment in Spain. However, studies on soil crusting were conducted separately to determine the differences between vegetation cover and bare or fallow conditions (Neave and Rayburg 2007; Ries and Hirt 2008; Gabriel et al. 2021), as well as various tillage treatments (Usón and Poch 2000; Wu et al. 2016; Ramos et al. 2019). Yet, there is a knowledge gap on soil crusting effects on soil hydro-physical properties under different tillage and crop sequences.

Rainfall and irrigation events after tillage and sowing can induce changes on soil hydraulic properties during the growing season due to modification of soil surface, and crust formation. Pareja-Sánchez

et al. (2017), working on the same experimental field, found that the potential route of irrigation water and soil losses (by splashing and soil sealing) occurred between rows (B-row), and it was more evident in IT than in NT. They explained this was due to lack of vegetation cover B-row, and lack of crop residues on the soil surface during most part of the crop growing season when IT is used. Moreover, infiltration shows a highly dynamic behaviour during rainfall and irrigation events, intensity and time (Mubarak et al. 2009; Bador-reck et al. 2013). For instance, Mubarak et al. (2009) reported that, soil hydraulic conductivity reached a very low value at the end of irrigation period compared to initial under high frequency drip irrigation during a maize growing season. However, given the importance of soil surface crusting on soil water balance, most studies were conducted in rain-fed conditions (Moore and Singer 1990; Vandervaere et al. 1997; Baumhardt et al. 2004; Neave and Rayburg 2007; Ries and Hirt 2008; Alagna et al. 2013, 2019; Nciizah and Wakindiki 2014), with only a few undertaken under irrigated conditions (Gabriel et al. 2021).

In Mediterranean area, evapotranspiration in summer periods, with rising temperatures and lower precipitation, is mostly balanced by high-frequency water applications in newly irrigated areas. During the irrigation period, water supply would have to cover a growing water demand; hence, knowledge about crust development and associated impact on soil hydraulic properties over time is required to establish an appropriate irrigation plan preventing soil and water losses by overflow. This is especially important in non-flat areas with sprinkler irrigation systems. As a matter of fact, penetration resistance (PR) was measured in the same experimental field to characterized crust strength and it was reported that PR increased over time after tillage under IT and RT between row of crops (B-row). Beside this, PR was lower within the row of crops (W-row) and similar regardless of tillage treatment (Pareja-Sánchez et al. 2017). However, this previous study did not investigate the consequence of crusting on surface soil hydro-physical properties dynamics. Therefore, research concerning the effect of crusting on soil hydro-physical properties over time under different management practices in irrigation conditions is still scarce.

This study used the Beerkan Estimation of Soil Transfer (BEST) method (Lassabatère et al. 2006) to obtain the soil water characteristics from small shallow circular ponds transient infiltration measurements in a field with high-frequency sprinkler irrigation and 2% slope. The objectives of this investigation were to assess the effect of crust on (i) soil physical and hydrodynamic properties and (ii) its spatio-temporal variations under various tillage, crop sequences, and position with respect to the crop row.

Materials and methods

Experimental site and design

This research was carried out on a long-term field experiment (26 years) in Agramunt, NE Spain (41°48′ N, 1°07′ E, 330 m asl). The climate of the area is semiarid Mediterranean, with 401 mm mean annual precipitation and 14.1 °C mean temperature. The soil has a 2% slope and was classified as Typic Xerofluvent according to USDA (Soil Survey Staff 2014). The upper (0–5 cm) horizon has a silt loam texture (Ramos et al. 2019). Other soil properties were pH (H_2O, 1:2.5): 8.5 and electrical conductivity (1:5): 0.15 dS m^{-1} (Cantero-Martínez et al. 2003).

The field was established in 1996 to compare three tillage systems, intensive tillage (IT), reduced tillage (RT), and no-tillage (NT), as well as three levels of mineral nitrogen (zero, medium, and high), with a single crop (barley) grown under rain-fed conditions (Angás et al. 2006). In 2015, a solid set sprinkler irrigation system was installed in the experimental field and transformed to irrigated conditions (Pareja-Sánchez et al. 2017).

Crop sequence was added as a factor in 2018 and it has two levels: short-term fallow-maize (Zea mays L.) (FM) and legume (pea; Pisum sativum L. or vetch; Vicia sativa L.)-maize (LM). Summer and winter crops, respectively, were maize and legume. A split-plot with three replications was used for the experimental design (three blocks). The tillage plots were 50 m long and 6 m in width, and the crop sequence plots were 50 m long and 3 m in width. The present work was done in 2020–21, during the third year after introducing the crop sequences, using vetch as winter crop for LM. Only the plots under medium fertilization rate were included in the experiment. Soil organic carbon concentration (0–5 cm depth) was 21.1, 14.8 and 10.3 g C kg^{-1} soil for NT, RT and CT, respectively (Pareja-Sánchez et al. 2017).

On the IT and RT plots, tillage was performed twice: autumn and spring. Autumn tillage was done

on the same day for both FM and LM, however spring tillage took place before planting maize at different times, one month earlier for FM (late maturing maize) than for LM (early maturing maize) (Fig. 1). In IT plots, autumn tillage consisted of a subsoiler pass (depth: 35 cm) followed by a chisel (depth: 15 cm) (which helped to incorporate crop residues into the soil nearly 100%) and a roller (to make the surface even). The spring tillage consisted of a rototiller (15 cm depth) followed by a chisel pass and a roller. In contrast, RT plots had similar tillage practices in both autumn and spring, a chisel pass (15 cm depth) and a roller. In NT plots, glyphosate spraying was done prior to planting. In the three tillage systems, vetch and maize were both planted using the pneumatic row direct drilling machine. Double disc furrow openers were used to make the slots, and rotary residue row cleaners were used to clear the path for the opening of the row unit.

Irrigation was scheduled weekly using the crop evapotraspiration (ETc) estimations of the Department of Agriculture of the Generalitat de Catalunya for the specific site, crops and growing stage. Due to the irrigation system design constrains, every irrigation sector included plots with different crops or growing stages, and the irrigation doses were selected according to the most demanding crop. During 2018–19, the irrigation dose was applied in one event per day, and water losses by runoff were observed, especially in IT. Then, from 2019–20, the irrigation dose was split in two events per day to reduce runoff.

Maximum daily irrigation dose was 90 m^3 ha^{-1}, and the precipitation rate of the sprinklers 6 mm h^{-1} (Christiansen Uniformity Coefficient: 78.10). Irrigation water comes from a snow-fed river's dam, which explain its low EC (0.237 dS/m) and SAR is also low (0.30). According to Ayers and Westcot (1985), with these values, there is no risk of reduced water availability nor toxicity for the plants, but irrigation water can have a slight to moderate effect on infiltration rate.

Vetch was mowed as fodder, and maize was harvested using a commercial combine harvesting machine. After harvesting, the residue was chopped and spread over the soil surface.

Soil sampling and infiltration measurements

A total of 180 infiltration runs covering approximately a total of 318 m^2 were carried out at five sampling times, with two runs per plot. The first three samplings were done 18, 60, and 137 days after the autumn tillage (30 November 2020), while vetch was grown in LM and FM was left fallow (Table S1 and Fig. 1). The last two samplings were conducted 63, and 205 (FM)/177 (LM) days after the spring tillage (21 April 2021 for FM, and 19 May 2021 for LM). LM plots had two distinct positions for the infiltration runs: W-row, and B-row. Similarly, FM plots had two samplings, during the fallow period, when there was no distinguishable position.

Infiltration runs were carried out with the Beerkan method following Lassabatère et al. (2006). Briefly,
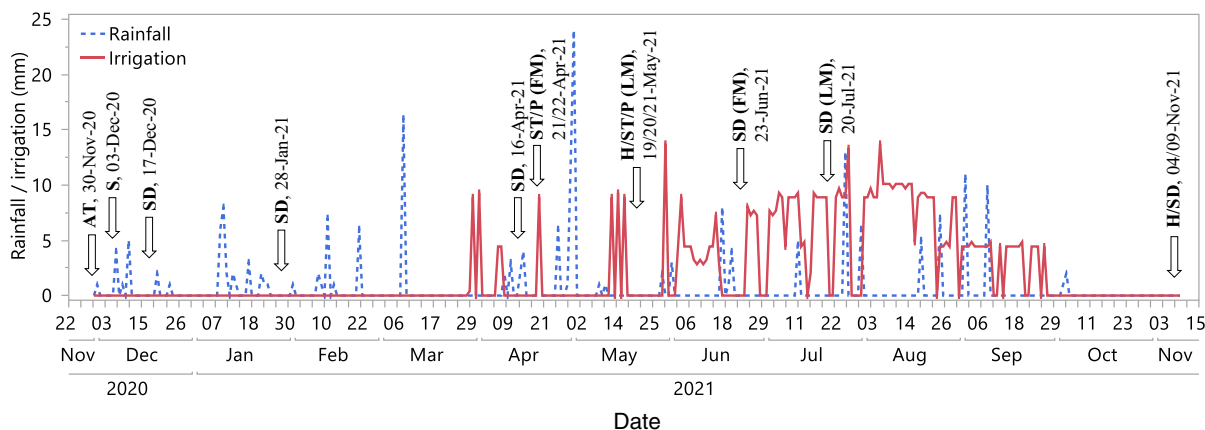
Fig. 1 Rainfall or irrigation (mm day^{-1}) during the experimental year (2020–21). Arrows represent key dates of management practice and sampling (AT, autumn tillage; S, sowing vetch, SD; sampling date, ST, spring tillage; P, planting maize; H, harvesting)

at every infiltration run, a stainless-steel ring of known inner diameter (135 or 150 mm) and height (100 mm) was installed on a relatively flat place. The ring was inserted into the soil surface a shallow depth (approximately 10 mm) to avoid lateral losses of water. In case of RT and NT, the crop residue and litter were removed prior to ring installation. Initial soil water content ranged between 0.17–0.29 cm^3 cm^{-3}, which helped to prevent crust alteration during ring installation. When soil surface was too dry, before ring installation, a syringe was used to introduce some water to the ring wall to avoid crust breakdown. Then, known volumes of water, usually 100 mL, were repeatedly poured into the ring, and the elapsed time to complete infiltration recorded. To reduce the possibility of crust alteration, water was added from a close distance at low rate. The time to infiltrate was increasing with each pouring. In some cases, when filtration was low owing to the crust and time to infiltrate was too long, the volume of water poured was reduced from 100 to 50 mL. This adjustment helped to obtain enough points of the cumulative infiltration curve for fitting the BEST algorithms. The infiltration test was continued until the difference in infiltration time between successive pouring's was negligible, indicating essentially steady-state infiltration, or until a pre-determined amount of water pouring's, never less than eight, were applied (Lassabatère et al. 2006). Additionally, soil samples (0- 0.05 m depth) were collected close to the point of infiltration runs to determine the dry soil bulk density, ρ_b and initial soil water content, θ_0. The bulk density (g cm-3) was calculated as the ratio of oven-dried soil mass (g) to soil bulk volume (cm3). To obtain oven-dried soil mass, the core soil (diameter: 0.06 m, and height: 0.05 m) was dried at 105 °C for 24 h. Soil water content was determined gravimetrically and multiplied by ρ_b to obtain volumetric soil water content.

To determine soil hydraulic properties, the BEST algorithms were used (Lassabatère et al. 2006). BEST algorithms determine the soil water retention curve $\theta(h)$ using the van Genuchten (1980) equation (Eq. (1a)), and the hydraulic conductivity function $K(\theta)$ using the Brooks and Corey (1964) equation (Eq. 2a), following Burdine (1953) conditions (Eq. 1b) and (Eq. 2b), respectively.

$$\frac{\theta - \theta_r}{\theta_s - \theta_r} = \left(1 + \left(\frac{h}{h_g}\right)^n\right)^{-m} \tag{1a}$$

$$m = 1 - \frac{2}{n} \tag{1b}$$

$$\frac{K(\theta)}{K_s} = \left(\frac{\theta - \theta_r}{\theta_s - \theta_r}\right)^\eta \tag{2a}$$

$$\eta = \frac{2}{mn} + 2 + p \tag{2b}$$

where θ_r and θ_s are the residual and saturated volumetric water content (cm^3 cm^{-3}), respectively; n and m are shape parameters, and h_g is the pressure head scale parameter (mm) representing the inflexion point of the water retention curve $\theta(h)$, K_s is the saturated hydraulic conductivity (mm s^{-1}) and η is the shape parameter of the soil hydraulic conductivity function $K(\theta)$; p is the tortuosity factor set equal to 1 when the m and n relationship is described by Eq. 1b. According to Haverkamp et al. (2006), shape parameters n, m, and η are dependent on soil texture (soil management practices would not change those parameters), whilst θ_s, K_s, and h_g are scaling parameters dependent on soil structure (soil management practices would change those parameters).

In BEST, the θ_r is assumed to be zero. The θ_s was assumed to equal total porosity that was estimated from soil bulk density and soil mineral particles density (2.65 g cm^{-3}). The n parameter was computed from soil sand (>0.05 mm) and clay (<0.002 mm) percent (Minasny and McBarney 2007) which were 22.5% and 13.7% in block 1, 29.9% and 11.7% in block 2, and 41.6% and 9.5% in block 3, and m and η from Eq. (1b) and (2b) respectively.

The h_g shape parameter was estimated by the following relationship:

$$h_g = -\frac{S^2}{C_p(\theta_s - \theta_0)\left[1 - \left(\frac{\theta_0}{\theta_s}\right)^\eta\right]K_s} \tag{3}$$

where S (mm $s^{-0.5}$) and θ_r (cm^3 cm^{-3}) are the soil sorptivity and initial soil water content, respectively. C_p is a coefficient dependent on n, m, and η (Lassabatère et al. 2006), and hence on soil texture. In BEST, S and K_s are estimated by fitting the Haverkamp's three-dimensional infiltration model (Haverkamp et al. 1994) to the experimental infiltration data.

Three alternative BEST algorithms are used i.e., BEST-slope (Lassabatère et al. 2006), that uses the slope of the regression of the last points (steady-state) to link S and K_s before fitting the transient model to the cumulative infiltration data while optimizing S, BEST-intercept (Yilmaz et al. 2010), that uses the intercept instead of the slope of the regression of the last points (steady-state) to link S and K_s before optimizing S with the transient data, and BEST-steady (Bagarello et al. 2014), that uses both the intercept and the slope of the regression of the last points (steady-state) to estimate S and K_s without fitting the transient state. All three fittings were done using the workbook from Di Prima (2013), available at https://bestsoilhydro.net/downloads/. Lassabatère et al. (2019) recommended to combine the estimates of all three algorithms. However, the BEST-slope algorithm results were not considered to estimate soil hydraulic parameters in this experiment because it failed to converge most of the times, particularly for crusted soil (Angulo-Jaramillo et al. 2019). Then, the results from the BEST-intercept and the BEST-steady algorithms were averaged to obtain the scale parameters θ_s, S, and K_s before statistical analysis.

Using capillary theory (Philip 1987), the "mean" characteristic pore size (radius) can be obtained from the following equation (Mubarak et al. 2009):

$$r = -\frac{2\sigma\mathrm{COS}\beta}{\rho g \alpha_h} \tag{4}$$

where σ is the soil–water surface tension (MT^{-2}), ρ is the density of water (ML^{-3}), g is the acceleration due to gravity (LT^{-2}), β is the contact angle between the water and the pore wall (assumed to be 0) and α_h is the capillary length (mm). The r (Eq. 4) represents the mean dimeter of pores that are hydraulically functional at the time of infiltration. As r increases, capillary forces decrease, and gravity forces progressively dominate the infiltration process.

α_h was calculated from the following simplified equation proposed by Di Prima et al. (2020).

$$\alpha_h = 0.861\frac{b_s}{\Delta\theta} \tag{5}$$

where b_s is the intercept of the linear regression obtained from the steady-state portion of the cumulative infiltration curve. $\Delta\theta$ is the difference between saturated (θ_s) and initial (θ_i) soil water content. The α_h indicates the relative magnitude of capillary and

gravity forces ($\alpha_h > 1000$ mm capillarity forces dominant, $\alpha_h < 10$ gravity forces dominant) that were present at the time of infiltration process from initial (θ_i) to saturated (θ_s) soil water content (Angulo-Jaramillo et al. 2000).

The number of effective pores N per unit area (m^{-2}), was calculated according to Watson and Luxmoore (1986), using r values and the Poiseuille equation:

$$N = \frac{8\mu K_s}{\pi\rho g r^4} \tag{6}$$

where μ is the dynamic viscosity of water ($ML^{-1}T^{-1}$). The N illustrates the number of hydraulically active pores present per unit area.

Statistical analysis

All the statistical analyses were done with the statistical package JMP Pro 16 (SAS Institute Inc, 2022). Data were checked for distribution (normality) and homogeneity of variance by the Shapiro-Wilk test and the Levene test, respectively. Variables such as S, Ks, r and N were Box-Cox-transformed before analysis. An analysis of variance (ANOVA) was performed for measured (ρb and $\theta 0$) and estimated (θs, S, Ks, r, and N) data to test the treatment (main) and their interactions effects. According to Federer and King (2007), sampling times were taken into account for main plot, following subplots included tillage systems and crop sequences. When the effects of treatments or interactions were significant, Student's t-tests were used to compare means at the 0.05 level of significance.

Results

The amount of rainfall + irrigation that was received on 18, 60, and 138 days after autumn tillage, was the same for LM and FM: $11 + 0 = 11$ mm, $29 + 0 = 29$ mm, and $45 + 27 = 72$ mm, respectively (Fig. 1). After the spring tillage, a varying amount of rainfall + irrigation was received by FM and LM, notably on 63 days, FM: $63 + 102 = 165$ mm, and LM: $23 + 242 = 265$ mm; 205/177 days, FM: $60 + 565 = 625$ mm, and LM: $55 + 398 = 453$ mm.

Bulk density

A significant interaction was observed between DAT and crop sequence ($p = 0.005$) on bulk density (ρ_b)

(Table 1). ρ_b changed over time and significant differences between crop sequences were observed after autumn and spring tillage. LM had higher ρ_b at 18 days after autumn tillage, whilst lower ρ_b at 63 days after spring tillage, compared to FM (Fig. 2).

ρ_b differences between the two positions considered, W-row and B-row, were always significant in LM ($p = 0.0003$) and FM ($p = 0.0001$) (Table 2). W-row had lower ρ_b compared to B-row (1.25 vs. 1.35 g cm^{-3} in LM, and 1.25 vs. 1.37 g cm^{-3} in FM).

Initial soil water content

Initial soil water content (θ_0) was significantly affected by DAT ($p < 0.001$) and tillage ($p < 0.001$) but not by crop sequences (Table 1). After autumn tillage at 60 days and spring tillage at 63 days, the highest (0.29 cm^3 cm^{-3}) and the lowest (0.17 cm^3 cm^{-3}) θ_0 were observed, respectively (Table 3). From highest to lowest, θ_0 followed the order NT > RT > IT (0.30, 0.22, and 0.19 cm^3 cm^{-3}, respectively) (Table 3). No significant interaction
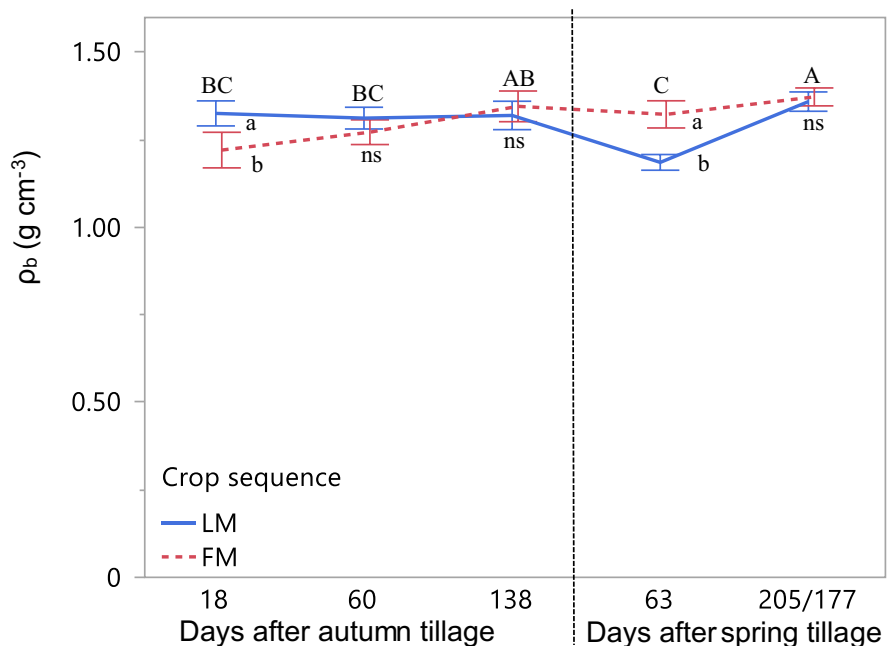
Table 1 ANOVA (p-values) of soil bulk density (ρ_b, g cm^{-3}), initial soil water content (θ_0, cm^3 cm^{-3}), sorptivity (S, mm s$^{-0.5}$), saturated hydraulic conductivity (K_s, mm s^{-1}), mean pore size (r, mm) and number of pores per unit area (N, m^{-2}) affected by days after autumn (18, 60, 138 days) and spring tillage (63, 205 and 177 days for FM and LM, respectively), tillage systems (IT: intensive tillage, RT: reduced tillage, and NT: no-tillage), crop sequences (FM: fallow-maize, LM: legume-maize) and their interactions

Source of variation	ρ_b (g cm^{-3})	θ_0 (cm^3 cm^{-3})	S * (mm s$^{-0.5}$)	K_s * (mm s^{-1})	r * (mm)	N * (m^{-2})
Days after tillage (DAT)	0.004	<.0001	0.0002	0.0003	<.0001	<.0001
Tillage (Till.)	<.0001	<.0001	<.0001	<.0001	0.005	0.0003
DAT *Till.	NS	NS	<.0001	<.0001	0.002	0.0006
Crop sequence (CS)	NS	NS	NS	NS	NS	NS
DAT *CS	0.005	NS	NS	NS	NS	NS
Till. * CS	NS	NS	0.03	NS	NS	NS
DAT *Till. *CS	NS	NS	NS	NS	NS	NS

*, data were BoxCox transformed before analysis; NS, non-significant at $p > 0.05$

Fig. 2 Bulk density (ρ_b, g cm^{-3}) dynamics at different days after autumn and spring tillage under two crop sequences (FM: fallow-maize, LM: legume-maize). Error bars show the standard error. Vertical dashed line separates the days after autumn and spring tillage. Different letters (uppercase letters among days after tillage and lowercase letters between crop sequences within each sampling date) indicate significant differences between treatments at $p < 0.05$; ns, non-significant

Table 2 Means' comparisons of soil bulk density (ρ_b, g cm^{-3}), initial soil water content (Θ_0, cm^3 cm^{-3}), sorptivity (S, mm s$^{-0.5}$), saturated hydraulic conductivity (K_s, mm s^{-1}), mean pore size (r, mm) and number of pores per unit area (N, m^{-2}) for two positions (W-row: within the crop row, B-row: between crop rows)

Factors	Levels	ρ_b (g cm^{-3})	Θ_0 (cm^3 cm^{-3})	S * (mm s$^{-0.5}$)	K_s * (mm s^{-1})	r * (mm)	N * (m^{-2})
LM (all sampling time had distinguished position)							
Position	B-row	1.35 a	0.24 a	0.38 b	0.009 b	0.20 a	6.90×10^7 b
	W-row	1.25 b	0.22 b	0.65 a	0.021 a	0.20 a	7.88×10^7 a
p value		0.0003	0.04	0.0003	0.0001	NS	0.0003
FM (after spring tillage, FM had distinguished position at 63 and 205/177 days)							
Position	B-row	1.37 a	0.22 a	0.37 b	0.005 b	0.17 a	7.68×10^7 b
	W-row	1.25 b	0.20 b	0.66 a	0.015 a	0.17 a	8.02×10^7 a
p value		0.0001	0.02	0.0004	0.001	NS	0.005

*, data were BoxCox transformed before analysis; different letters within the column indicate significant differences between treatments at $p < 0.05$

was observed among days after tillage (DAT), tillage, and crop sequences.

The difference between the two positions was always significant ($p = 0.04$ in LM, $p = 0.02$ in FM) (Table 2). W-row θ_0 was lower than the B-row (0.22 vs. 0.24 cm^3 cm^{-3} in LM, and 0.20 vs. 0. 22 cm^{-3} cm^3 in FM).

Sorptivity

A significant interaction between DAT and tillage ($p < 0.0001$), and between tillage and crop sequence ($p = 0.03$) were observed on sorptivity (S) (Table 1). Apart from 205/177 days after spring tillage (Fig. 3), the differences between IT

Table 3 Means' comparisons of soil bulk density (ρ_b, g cm^{-3}), initial soil water content (Θ_0, cm^3 cm^{-3}), sorptivity (S, mm s$^{-0.5}$), saturated hydraulic conductivity (K_s, mm s^{-1}), mean pore size (r, mm) and number of pores per unit area (N, m^{-2}) for different days after autumn and spring tillage, three tillage systems (IT: intensive tillage, RT: reduced tillage, and NT: no-tillage) and two crop sequences (FM: fallow-maize, LM: legume-maize). Amount of rainfall and irrigation (mm) received between two consecutive samplings

Factors	Levels	ρ_b (g cm^{-3})	Θ_0 (cm^3 cm^{-3})	S * (mm s$^{-0.5}$)	K_s * (mm s^{-1})	r * (mm)	N * (m^{-2})	Rainfall (mm)	Irrigation (mm)
Days after tillage									
Autumn tillage									
	18	1.27 bc	0.25 b	0.62 ab	0.018 ab	0.18 bc	8.43×10^7 a	11	0
	60	1.29 bc	0.29 a	0.66 a	0.020 a	0.14 c	8.95×10^7 a	29	0
	138	1.33 ab	0.20 c	0.39 c	0.016 b	0.37 a	6.17×10^7 b	45	27
Spring tillag	63 (FM) (LM)	1.25 c	0.17 d	0.55 ab	0.013 b	0.28 ab	7.05×10^7 b	63 / 23	102 / 242
	205 (FM) 177 (LM)	1.37 a	0.25 b	0.43 b	0.007 c	0.11 d	9.21×10^7 a	60 / 55	565 / 398
Tillage	IT	1.30 b	0.19 c	0.44 c	0.010 b	0.29 a	6.83×10^7 b		
	RT	1.23 c	0.22 b	0.67 a	0.018 a	0.19 b	8.38×10^7 a		
	NT	1.38 a	0.30 a	0.47 b	0.015 a	0.16 b	8.68×10^7 a		
Crop sequence	FM	1.31 a	0.24 a	0.57 a	0.015 a	0.21 a	8.10×10^7 a		
	LM	1.30 a	0.23 a	0.48 a	0.014 a	0.22 a	7.83×10^7 a		

*, data were BoxCox transformed before analysis; different letters within the column indicate significant differences between treatments at $p < 0.05$

and NT on S were substantially greater, as they were changes over time. On the other hand, RT showed little variation on S over time. Differences between LM and FM on S were only significant under NT (Table 1 and Fig. 4), with greater values for FM compared to LM.

Position always had a significant effect on S ($p=0.0003$ in LM, $p=0.0004$ in FM) (Table 2). W-row S was remarkably greater than B-row (0.65 vs. 0.38 mm s$^{-0.5}$ in LM, and 0.66 vs. 0.37 mm s$^{-0.5}$ in FM).

Saturated hydraulic conductivity

A significant interaction between DAT and tillage was observed on saturated hydraulic conductivity (K_s) (Table 1). Regardless of the tillage systems, K_s experienced significant changes over time (Fig. 3). IT increased K_s from 18 days after the autumn tillage up to 60 days, then decreased to 138 days and maintained similar or slightly higher K_s after the spring tillage. RT maintained a high K_s after the autumn tillage, which decreased remarkably after the spring tillage. NT had lower K_s at 18 and 60 days after the autumn sowing, then increased K_s until 138 days. K_s was maintained

up to 63 days after the spring sowing and then decreased to 205/177 days.

The effect of position on K_s was always significant in LM ($p=0.0001$), and FM ($p=0.001$) (Table 2). W-row K_s was greater compared to B-row (0.021 vs. 0.009 mm s^{-1} in LM, and 0.015 vs. 0.005 mm s^{-1} in FM).
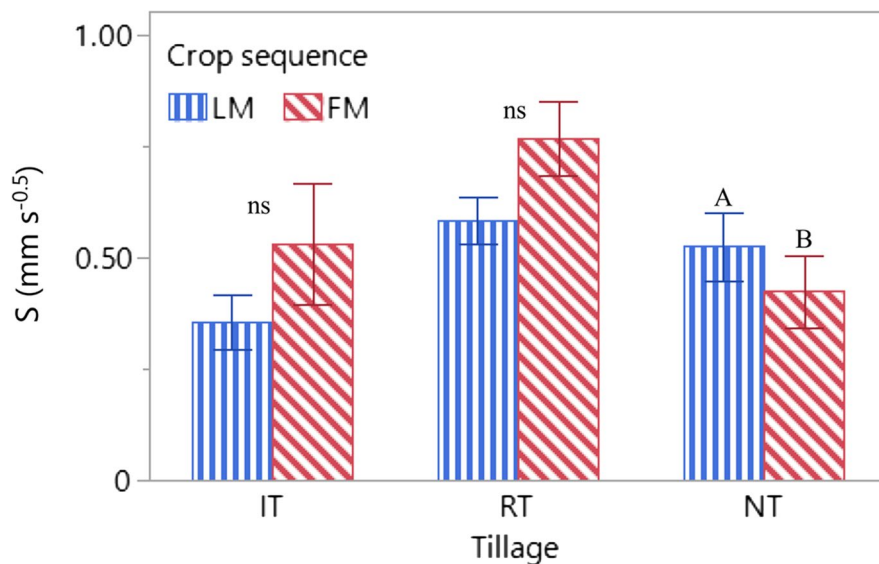
Mean pore size and number of pores per unit area

A significant interaction was observed between DAT and tillage on mean pore size (r, mm) ($p=0.002$) and number of pores per unit area (N, m^{-2}) ($p=0.0006$) (Table 1). Regardless of tillage, r and N varied greatly with time, especially in IT (Fig. 5). Both IT and RT showed lower and relatively similar r at 18 and 60 days after the autumn tillage, then increased at 138 days, maintaining this high value up to 63 days after the spring tillage, decreasing later on up to 205/177 days. On the contrary, N was found higher at 18 and 60 days after the autumn tillage, then decreased at 138 days, was maintained, or even slightly increased at 63 days after spring tillage and increased again at 205/177 days. NT showed greater r at 18, 60, and 138 days after the autumn sowing, then decreased slowly up to 205/177 days after the spring sowing. On the other hand,


Fig. 3 Sorptivity (**a**) (S, mm s$^{-0.5}$) and saturated hydraulic conductivity (**b**) (K_s, mm s^{-1}) dynamics at different days after tillage and tillage systems (IT: intensive tillage, RT: reduced tillage, and NT: no-tillage). Error bars show the standard error. Vertical dashed line separates the days after autumn and spring tillage. Different letters (uppercase letters among days after tillage and lowercase letters among tillage systems within each sampling date) indicate significant differences between treatments at $p < 0.05$; ns, non-significant
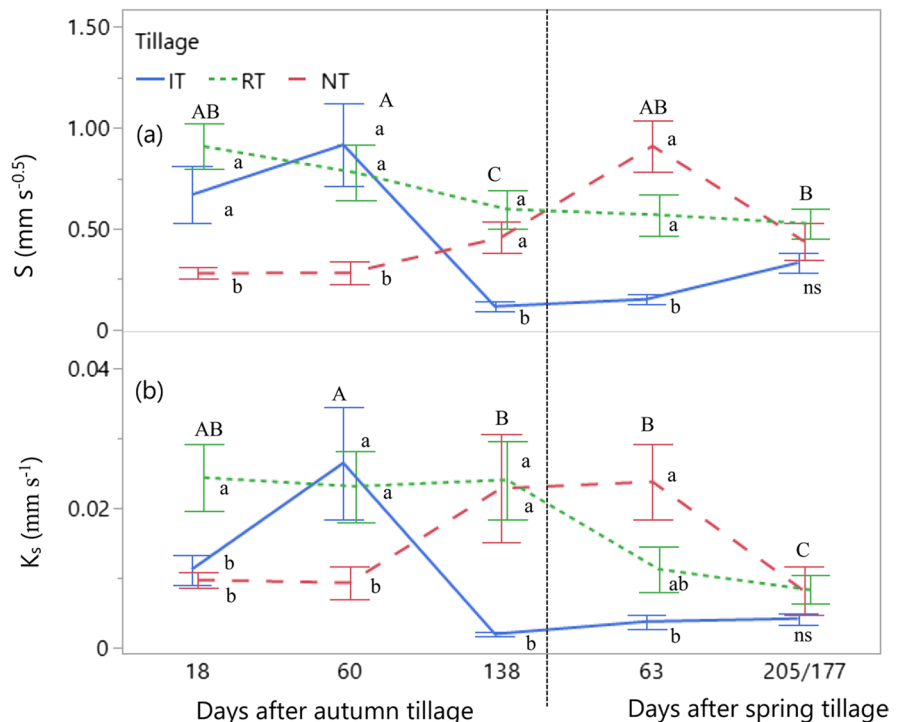
Fig. 4 Sorptivity (S, mm s$^{-0.5}$) under different tillage (IT: intensive tillage, RT: reduced tillage, and NT: no-tillage) and crop sequences (FM: fallow-maize, LM: legume-maize) (different sampling times were averaged). Error bars show the standard error and different uppercase letters indicates significant differences between treatments at $p < 0.05$; ns: non-significant)

Fig. 5 Mean pore size (**a**) (r, mm) and number of pores per unit area (**b**) (N, m^{-2}) dynamics at different days after tillage and tillage systems (IT: intensive tillage, RT: reduced tillage, and NT: no-tillage). Error bars show the standard error. Vertical dashed line separates the days after autumn and spring tillage. Different letters (uppercase letters among days after tillage and lowercase letters among tillage systems within each sampling date) indicate significant differences between treatments at $p < 0.05$; ns, non-significant
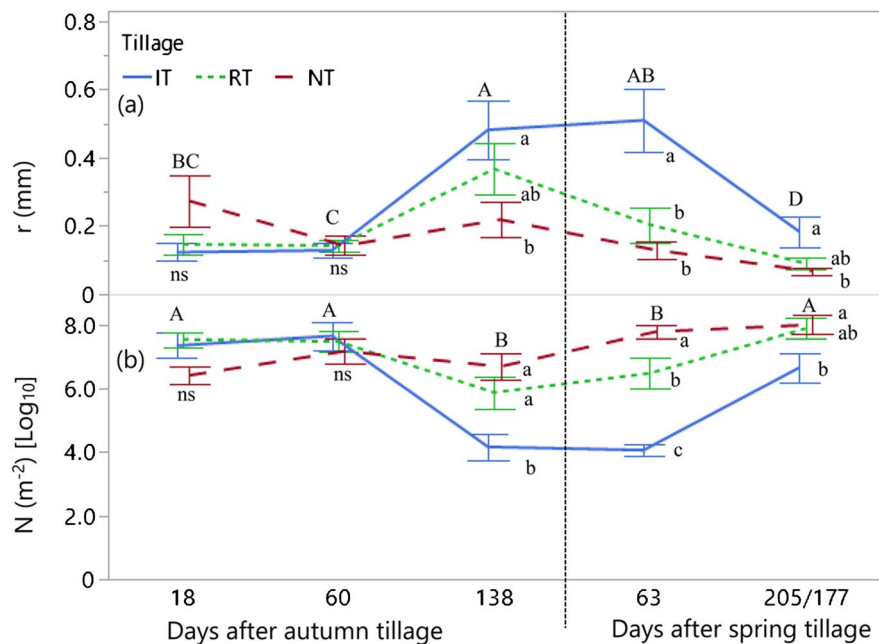
N increased slowly over time and reached its maximum at 205/177 days after spring sowing.

The effect of position was not significant on r but a significant effect was found on N ($p = 0.0003$ in LM, $p = 0.005$ in FM) (Table 2). Both B-row and W-row showed similar r (0.20 mm in LM, and 0.17 mm in FM) (Table 3). In addition, W-row had greater N compared to B-row (7.88×10^7 vs. 6.90×10^7 m^{-2} in LM, and 8.03×10^7 vs.7.68×10^7 m^{-2} in FM) (Table 2).

Discussion

Temporal variations of soil hydraulic properties

Temporal variations of soil hydraulic properties (S, K_s, r and N) caused by soil crust were great under IT and RT, less evident under long-term NT (Figs. 3 and 5), whilst no significant difference was observed between LM and FM (Tables 1 and 3). Figures 3 and

5, can be divided into two separate stages, viz., (i) 18, 60 and 138 days after autumn tillage, and (ii) 63 and 205/177 days after spring tillage. After the autumn tillage, IT showed an increasing trend on both S and K_s from 18 to 60 days, and then they declined and reached extremely low values at 138 days (Fig. 3). However, 63 and 205/177 days after spring tillage, IT showed mostly similar K_s values and slightly higher than 138 days after autumn tillage. Tillage, in general, alters the soil structure and pore systems, leading to the formation of macro-pores (Jirků et al. 2013). However, soil surface structure is expected to be fragile and unstable with regards to macro-pores (Feng et al. 2011). In this line clogging or blocking of the macro-pores could occur as a result of aggregate breakdown during rainfall or irrigation events (Ncii-zah and Wakindiki 2014). Tillage effects on S and K_s were easily mitigated, and variations on hydraulic properties occurred based on the rate and intensity of rainfall events and irrigation applications (Feng et al. 2011). The higher K_s that was observed at 18 and 60 days after autumn tillage could be attributed to macro-pores created by tillage, resulting in temporary increases in K_s. Besides this, in those two periods were received 11 and 29 mm of rainfall, respectively, with an intensity lower than 10 mm day^{-1} (Table 3, and Fig. 1). This amount of rainfall was not enough to form a strong crust to reduce K_s. On the contrary, an extremely low K_s value was recorded at 138 days after autumn tillage in IT because of crust formed by raindrops and irrigation application. This period received a total of 72 mm of rain and irrigation water, intensity of rain exceeded 10 mm day^{-1}, which was sufficient to form a seal and crust on the surface soil (Fig. 1). After the spring tillage, multiple rainfall and irrigation events with greater intensity (Fig. 1) developed a strong surface crust. As a consequence, tillage induced K_s and S enhancement were not found at 63 days after spring tillage, earlier than autumn tillage. In contrast, both K_s and S were reduced due to crust formation. Our results suggest that the crust development process was time-dependent, and was primarily governed by the overall rain or irrigation and their intensity (Figs. 1 and 3). Further, mean pore size (r) showed an increasing trend at 138 days after autumn tillage, whilst after spring tillage, found greater value at 63 days and then decreased at 205/177 days. In contrast, the opposite result was observed for number of pores per unit area (N). An increasing trend in pore size can be attributed by tillage operations, as well as biological activity and plant root development. At the same time mean pore size increased, the number of pores per unit area decreased greatly. This finding indicates that, although IT had greater r particularly at 138 and 63 days, it showed a lower value of K_s because of lower N. We hypothesized that lower N under those sampling date could be linked to poor connection between pores. In a study in the same experimental field, it was documented that due to lower pore continuity IT had similar gas diffusivity to NT, although IT had greater air-filled porosity than NT (Talukder et al. 2022).

After the autumn tillage, S and K_s did not change significantly under RT, whereas an increasing trend of r and a decreasing trend of N were observed over time. After the spring tillage, both S and K_s showed a decreasing trend over time. r showed a maximum value at 63 days and then declined. Again, N showed a lower value at 63 days and then increased slightly (Figs. 3 and 5). Rainfall and irrigation after autumn tillage were not enough to create a strong crust, and consequently, S and K_s were high up to 138 days in RT. After spring tillage, multiple rainfall and especially irrigation events following tillage quickly formed a strong crust, and as a consequence, K_s was low under RT from the beginning. Similarly, NT showed an increasing trend on S and K_s over time and then declined at the end (205/177). A slightly decreasing trend over time was observed for r, whereas N showed the opposite, an increasing trend. These findings illustrate that, with reduction of tillage intensity from IT to NT crust formation was lowered. It was well documented that long-term RT and NT formed a more stable soil structure than IT. As a result, RT and NT were more resilient to crust formation than IT. Due to less disturbance, Palese et al. (2014) found that the effect of crusting was lower under reduced (RT) and no-tillage (NT) compared to conventional tillage (IT) on semi-arid sandy loam soils. Because of the occurrence of crusting and compacted layers in IT, they observed lower infiltration of rainfall water. In addition, findings of this study are supported by the previous studies conducted in the same experimental field indicating that the soil structure was improved under NT compared to RT and IT (Pareja-Sánchez et al. 2017; Talukder et al. 2022). In these studies, soil physical properties such as gas diffusivity, and

macropore continuity were greater under NT than IT (Talukder et al. 2022), the macroaggregates water stability was lower under IT and RT due to decreased soil orgaic content than NT (Pareja-Sánchez et al. 2017). Notwithstanding, the results of the surface runoff and sediment yield measurements made over the course of 2018–19 to 2020–21 in the same study area revealed that crusting impacts based on tillage practice. It was demonstrated that regardless of the year, surface runoff and sediment yield were greater under IT and RT than NT (unpublished work). Beside this, some other possible reasons can be (i) IT (100%) incorporates greater quantity of crop residues into the soil than RT (70%), whereas crop residues remain in NT (85%), (ii) crop establishment was delayed under IT and RT compared to NT (Pareja-Sánchez et al. 2017) and both biomass and grain yield were greater under RT and NT. Therefore, strong surface crust under IT could be attributed to lower surface cover by crop residues or living crops than RT and NT, making the soil aggregates exposed to water drop impact. Additionally, in the same study area (Cantero-Martínez et al. 2004) reported that greater activity of earthworms in the top soil (0–30 cm depth) of NT system than IT. We hypothesized that under conservation tillage, especially in NT channelling and burrowing by earthworms loosens the surface soil and creates preferential paths for infiltration and percolation of water. As a consequence, NT had greater hydraulic conductivity during the high frequency irrigation period. Moreover, both S and K_s were decreased 205/177 days after the spring tillage under NT. The reason can be that maximum amount of rainfall + irrigation (566 and 398 mm for FM and LM, respectively) was received during this period. In this line, Angulo-Jaramillo et al. (2000) reported soil hydraulic properties variation over time under two kinds of soils (sand and sandy loam). Under furrow irrigation, K_s values declined from the beginning of irrigation period towards the end. At the end of the irrigation period, both S and K_s showed lower values compared to the beginning of irrigation. Our results are consistent with Angulo-Jaramillo et al. (2000) and observed a similar trend.

In summary, raindrops and irrigation water following tillage contributed to settle down the fragile structure created by the tillage and developed surface crusting; consequently, temporal variation on S, K_s, r, and N due to tillage did not persist over a long time.

Beside this, multiple rainfall events and irrigation applications and their intensities were capable to create a strong crust. The negative effects of soil crust on S and K_s were greater under IT than RT, and little under long-term NT. Nevertheless, the effect of crust on temporal variation of soil hydraulic properties was potentially greater at the end of irrigation period and less at the beginning of irrigation particularly under RT and NT.

Spatial variations of soil hydraulic properties

The saturated hydraulic conductivity (K_s) was around three times higher W-row than B-row in FM and LM (Table 2). The difference in K_s values was due to crust formation and was more prominent B-row. Seeding or row planting (W-row) is insufficient to cover the whole soil surface, especially during the vegetative stage of crops, which exposes more soil surface to water drop impact. The presence of the crops W-row, led to the weakening or lowering of crust development by intercepting raindrops and irrigation water, and reducing the falling energy when reaching the surface (Neave and Rayburn 2007). In contrast, B-row was directly exposed to rain or irrigation water and formed a well-developed crust. Furthermore, plant roots strengthened the stability of surrounding aggregates by decaying roots biomass at the W-row, leading to a reduction in aggregate physical dispersion and transportation caused by water action (Fageria and Stone 2006). This last process is aggravated by the presence of soil sediment prevailed in between rows of crops, particularly under IT as observed by Pareja-Sánchez et al. (2017) in the same field. Several authors working under different environmental conditions found similar results (Alagna et al. 2019; Neave and Rayburg 2007; Ries and Hirt 2008; Souza et al. 2014). For instance, Alagna et al. (2019) reported that B-row areas had lower K_s (by a factor of 1.6) than W-row due to crust formation under rainfed Mediterranean vineyard loamy soils. In addition, it was observed that W-row had lower bulk density (ρ_b), and a higher number of hydraulically active pores per unit area (N), with the same pore size, (r) than B-row (Table 2). This indicates that the W-row was more conductive due to an increased number of pores per unit area. Our results match with the results of Souza et al. (2014) who used BEST method in a Brazilian Oxisol cultivated with castor bean (*Ricinus*

communis L.). They found that non-crusted (W-row) soils were 3 times more conductive (K_s) than crusted soils (B-row) due to higher number of hydraulically active pores per unit area, and also recorded lower bulk density for non-crusted soils. Moreover, Jirků et al. (2013) reported that K_s increased proportionally with θ_s, whereas decreased inversely in relation to ρ_b. Our results showed a similar pattern; a negative relation between ρ_b and K_s was observed B-row (greater ρ_b and lower K_s).

Likewise, K_s, sorptivity (S) was always significantly higher W-row, around 1.70 times higher than B-row. S represents how fast/readily a soil absorbs water at the initial stage of a rainfall event or irrigation application due to capillary force (Castellini et al. 2016). Our results suggested that presence of crust B-row impaired the soil's ability to infiltrate water compared to W-row, as Alagna et al. (2019) found. Castellini et al. (2016) reported that S increased proportionally to soil organic content and was inversely related to ρ_b. Our results correspond the findings, exhibiting a negative relationship between ρ_b and S.

Conclusions

Two-fold higher hydraulic conductivity and sorptivity were found under the crop row compared to between rows because of greater number of pores per unit area. Between rows soil remain unprotected in the first stages of the crop development, highlight the protective effect of the crop canopy on the soil that prevents crusting. Furthermore, this preferential water flow path should not be neglected when conducting infiltration experiments in row crops, or at least the sampling position must be indicated when comparing results.

The initial enhancements of porosity by intensive tillage, are lost very easily in the short-term because of weak structural stability of surface soil which becomes prone to crust formation. This surface crusting leads to decrease sorptivity, hydraulic conductivity and number of actively conducting pores. On the contrary, no-tillage and reduced tillage can be a management choice in Mediterranean areas, also under irrigated conditions, due to better structural stability. Structurally stable soils are resilient to crust formation, and enhanced soil hydraulic properties, which can improve the efficiency of rain and irrigation water use by reducing runoff. Incorporation of pea or vetch before maize lowered bulk density during the maize growing period, but it did not improve soil hydraulic properties after three years. Long-term impacts of legume-maize sequence on soil crusting needs to be assessed in future research. Finally, effects of crust should be considered while modelling or simulating soil water movement and/or scheduling irrigation.

References

Agassi M, Shainberg I, Morin J (1981) Effect of electrolyte concentration and soil sodicity on infiltration rate and crust formation. Soil Sci Soc Am J 45:848–851. https://doi.org/10.2136/sssaj1981.03615995004500050004x

Alagna V, Bagarello V, Di Prima S, Giordano G, Iovino M (2013) A simple field method to measure the hydrodynamic properties of soil surface crust. J Agric Eng 44:74–79. https://doi.org/10.4081/jae.2013.(s1):e14

Alagna V, Bagarello V, Di Prima S, Guaitoli F, Iovino M, Keesstra S, Cerdà A (2019) Using Beerkan experiments to estimate hydraulic conductivity of a crusted loamy soil in a Mediterranean vineyard. J Hydrol Hydromech 67:191–200. https://doi.org/10.2478/johh-2018-0023

Angás P, Lampurlanés J, Cantero-Martínez C (2006) Tillage and N fertilization: effects on N dynamics and Barley

yield under semiarid Mediterranean conditions. Soil Till-age Res 87:59–71. https://doi.org/10.1016/j.still.2005.02.036

Angulo-Jaramillo R, Vandervaere J-P, Roulier S, Thony J-L, Gaudet J-P, Vauclin M (2000) Field measurement of soil surface hydraulic properties by disc and ring infiltrom-eters. Soil Tillage Res 55:1–29. https://doi.org/10.1016/S0167-1987(00)00098-2

Angulo-Jaramillo R, Bagarello V, Di Prima S, Gosset A, Iovino M, Lassabatere L (2019) Beerkan Estimation of Soil Transfer parameters (BEST) across soils and scales. J Hydrol 576:239–261. https://doi.org/10.1016/j.jhydrol.2019.06.007

Assouline S (2004) Rainfall-induced soil surface sealing: a critical review of observations, conceptual models, and solutions. Vadose Zo J 3:570–591. https://doi.org/10.2136/vzj2004.0570

Ayers RS, Westcot DW (1985) Water quality for agriculture. FAO Irrigation and Drainage, Paper 29, Food and Agri-culture Organization, Rome

Badorreck A, Gerke HH, Hüttl RF (2013) Morphology of physical soil crusts and infiltration patterns in an artificial catchment. Soil Tillage Res 129:1–8. https://doi.org/10.1016/j.still.2013.01.001

Bagarello V, Di Prima S, Iovino M (2014) Comparing alterna-tive algorithms to analyze the Beerkan infiltration experi-ment. Soil Sci Soc Am J 78:724–736. https://doi.org/10.2136/sssaj2013.06.0231

Baumhardt RL, Unger PW, Dao TH (2004) Seedbed surface geometry effects on soil crusting and seedling emergence. Agron J 96:1112–1117. https://doi.org/10.2134/agronj2004.1112

Brooks RH, Corey AT (1964) Hydraulic Properties of Porous Media, Colorado State University Hydrology Paper. Colo-rado State University

Burdine NT (1953) Relative permeability calculations from pore size distribution data. J Pet Technol 5:71–78. https://doi.org/10.2118/225-G

Cantero-Martínez C, Angas P, Lampurlanés J (2003) Growth, yield and water productivity of barley (Hordeum vulgare L.) affected by tillage and N fertilization in Mediterra-nean semiarid, rainfed conditions of Spain. Field Crop Res 84:341–357. https://doi.org/10.1016/S0378-4290(03)00101-1

Cantero-Martínez C, Ojeda L, Ángas P, Santiveri P (2004) Téc-nicas de laboreo del suelo en zonas de secano semi-árido; Efecto sobre la población de lombrices. Departemento de Production Vegetal Y Ciencia Forestal, Universitat Lleida, ETSEA, pp 724–729

Castellini M, Iovino M, Pirastru M, Niedda M, Bagarello V (2016) Use of BEST procedure to assess soil physical quality in the Baratz lake catchment (Sardinia, Italy). Soil Sci Soc Am J 80:742–755. https://doi.org/10.2136/sssaj2015.11.0389

Chen L, Sela S, Svoray T, Assouline S (2013) The role of soil-surface sealing, microtopography, and vegetation patches in rainfall-runoff processes in semiarid areas. Water Resour Res 49:5585–5599. https://doi.org/10.1002/wrcr.20360

Di Prima S (2013) Automatic analysis of multiple Beerkan infiltration experiments for soil hydraulic characterization.

In Proceedings of the 1st CIGR Inter-Regional Confer-ence on Land and Water Challenges, Bari, Italy, pp 10–14

Di Prima S, Stewart RD, Castellini M, Bagarello V, Abou Najm MR, Pirastru M, Giadrossich F, Iovino M, Angulo-Jara-millo R, Lassabatere L (2020) Estimating the macroscopic capillary length from Beerkan infiltration experiments and its impact on saturated soil hydraulic conductivity pre-dictions. J Hydrol 589:125159. https://doi.org/10.1016/j.jhydrol.2020.125159

Fageria N, Stone L (2006) Physical, chemical, and biologi-cal changes in the rhizosphere and nutrient availability. J Plant Nutr 29:1327–1356. https://doi.org/10.1080/01904160600767682

Federer WT, King F (2007) Variations on split plot and split block experiment designs. John Wiley & Sons, Inc., Hoboken, NJ. https://doi.org/10.1002/0470108584

Feng G, Sharratt B, Young F (2011) Influence of long-term till-age and crop rotations on soil hydraulic properties in the US Pacific Northwest. J Soil Water Conserv 66:233–241. https://doi.org/10.2489/jswc.66.4.233

Gabriel JL, García-González I, Quemada M, Martin-Lammerd-ing D, Alonso-Ayuso M, Hontoria C (2021) Cover crops reduce soil resistance to penetration by preserving soil sur-face water content. Geoderma 386:114911. https://doi.org/10.1016/j.geoderma.2020.114911

Haverkamp R, Debionne S, Angulo-Jaramillo R, de Condappa D (2006) Soil properties and moisture movement in the unsaturated zone. In: Delleur JW (ed) The handbook of groundwater engineering. CRC, Boca Raton, pp 6.1 6.59. https://doi.org/10.1201/9781420006001

Haverkamp R, Ross PJ, Smettem KRJ, Parlange JY (1994) Three-dimensional analysis of infiltration from the disc infiltrometer. 2. Physically based infiltration equation. Water Resour Res 30:2931–2935. https://doi.org/10.1029/94WR01788

Jirků V, Kodešová R, Nikodem A, Mühlhanselová M, Žigová A (2013) Temporal variability of structure and hydraulic properties of topsoil of three soil types. Geoderma 204–205:43–58. https://doi.org/10.1016/j.geoderma.2013.03.024

Lassabatère L, Angulo-Jaramillo R, Soria Ugalde JM, Cuenca R, Braud I, Haverkamp R (2006) Beerkan estimation of soil transfer parameters through infiltration experiments-BEST. Soil Sci Soc Am J 70:521–532. https://doi.org/10.2136/sssaj2005.0026

Lassabatere L, Di Prima S, Angulo-Jaramillo R, Keesstra S, Salesa D (2019) Beerkan multi-runs for characterizing water infiltration and spatial variability of soil hydraulic properties across scales. Hydrol Sci J 64:165–178. https://doi.org/10.1080/02626667.2018.1560448

Minasny B, McBratney AB (2007) Estimating the water reten-tion shape parameter from sand and clay content. Soil Sci Soc Am J 71:1105–1110. https://doi.org/10.2136/sssaj2006.0298N

Moore DC, Singer MJ (1990) Crust formation effects on soil ero-sion processes. Soil Sci Soc Am J 54:1117–1123. https://doi.org/10.2136/sssaj1990.03615995005400040033x

Mubarak I, Mailhol JC, Angulo-Jaramillo R, Ruelle P, Boivin P, Khaledian M (2009) Temporal variability in soil hydraulic properties under drip irrigation. Geoderma

150:158–165. https://doi.org/10.1016/j.geoderma.2009.01.022

Nciizah A, Wakindiki I (2014) Rainfall intensity effects on crusting and mode of seedling emergence in some quartz-dominated South African soils. Water SA 40:587. https://doi.org/10.4314/wsa.v40i4.2

Neave M, Rayburg S (2007) A field investigation into the effects of progressive rainfall-induced soil seal and crust development on runoff and erosion rates: the impact of surface cover. Geomorphology 87:378–390. https://doi.org/10.1016/j.geomorph.2006.10.007

Palese AM, Vignozzi N, Celano G, Agnelli AE, Pagliai M, Xiloyannis C (2014) Influence of soil management on soil physical characteristics and water storage in a mature rainfed olive orchard. Soil Tillage Res 144:96–109. https://doi.org/10.1016/j.still.2014.07.010

Pareja-Sánchez E, Plaza-Bonilla D, Ramos MC, Lampurlanés J, Álvaro-Fuentes J, Cantero-Martínez C (2017) Long-term no-till as a means to maintain soil surface structure in an agroecosystem transformed into irrigation. Soil Tillage Res 174:221–230. https://doi.org/10.1016/j.still.2017.07.012

Philip JR (1987) The quasi-linear analysis, the scattering analog, and other aspects of infiltration and seepage. In: Fok YS (ed) Infiltration development and application. Water Resources Research Center, Honolulu, pp 1–27

Ramos MC, Pareja-Sánchez E, Plaza-Bonilla D, Cantero-Martínez C, Lampurlanés J (2019) Soil sealing and soil water content under no-tillage and conventional tillage in irrigated corn: effects on grain yield. Hydrol Process 33:2095–2109. https://doi.org/10.1002/hyp.13457

Ries JB, Hirt U (2008) Permanence of soil surface crusts on abandoned farmland in the Central Ebro Basin/Spain. CATENA 72:282–296. https://doi.org/10.1016/j.catena.2007.06.001

Šimůnek J, Angulo-Jaramillo R, Schaap MG, Vandervaere J-P, van Genuchten MT (1998) Using an inverse method to estimate the hydraulic properties of crusted soils from tension-disc infiltrometer data. Geoderma 86:61–81. https://doi.org/10.1016/S0016-7061(98)00035-4

Soil Survey Staff (2014) Keys to soil taxonomy, 12th edn. USDA-Natural Resources Conservation Service, Washington, DC

Souza ES, Antonino ACD, Heck RJ, Montenegro SMGL, Lima JRS, Sampaio EVSB, Angulo-Jaramillo R, Vauclin M (2014) Effect of crusting on the physical and hydraulic properties of a soil cropped with Castor beans (Ricinus communis L.) in the northeastern region of Brazil. Soil Tillage Res 141:55–61. https://doi.org/10.1016/j.still.2014.04.004

Talukder R, Plaza-Bonilla D, Cantero-Martínez C, Wendroth O, Castel JL (2022) Soil gas diffusivity and pore continuity dynamics under different tillage and crop sequences in an irrigated Mediterranean area. Soil Tillage Res 221:105409. https://doi.org/10.1016/j.still.2022.105409

Usón A, Poch RM (2000) Effects of tillage and management practices on soil crust morphology under a Mediterranean environment. Soil Tillage Res 54:191–196. https://doi.org/10.1016/S0167-1987(99)00099-9

van Genuchten (1980) A closed-form equation for predicting the hydraulic conductivity of unsaturated soils. Soil Sci Soc Am J 44:892–898

Vandervaere J-P, Peugeot C, Vauclin M, Angulo Jaramillo R, Lebel T (1997) Estimating hydraulic conductivity of crusted soils using disc infiltrometers and minitensiometers. J Hydrol 188–189:203–223. https://doi.org/10.1016/S0022-1694(96)03160-5

Watson KW, Luxmoore RJ (1986) Estimating macroporosity in a forest watershed by use of a tension infiltrometer. Soil Sci Soc Am J 50:578–582. https://doi.org/10.2136/sssaj1986.03615995005000030007x

Wu Q, Wang L, Wu F (2016) Effects of structural and depositional crusts on soil erosion on the Loess Plateau of China. Arid l Res Manag 30:432–444. https://doi.org/10.1080/15324982.2016.1157837

Yilmaz D, Lassabatere L, Angulo-Jaramillo R, Deneele D, Legret M (2010) Hydrodynamic characterization of basic oxygen furnace slag through an adapted BEST method. Vadose Zo J 9:107. https://doi.org/10.2136/vzj2009.0039